Energetic Particle Radiation Environment Observed by RAD on the Surface of Mars during the September 2017 Event

B. Ehresmann[1], D. M. Hassler[1], C. Zeitlin[2], J. Guo[3], R. F. Wimmer-Schweingruber[3], D. Matthiä[4], H. Lohf[3], S. Burmeister[3], S. C. R. Rafkin[1], T. Berger[4] and G. Reitz[4]

Bent Ehresmann, ehresmann@boulder.swri.edu

[1]Southwest Research Institute, Boulder, CO, USA

[2]Leidos Innovations Corporation, Houston, TX, USA

[3]Christian-Albrechts-Universität zu Kiel, Germany

[4]Deutsches Zentrum für Luft- und Raumfahrt, Cologne, Germany

This article has been accepted for publication and undergone full peer review but has not been through the copyediting, typesetting, pagination and proofreading process, which may lead to differences between this version and the Version of Record. Please cite this article as doi: 10.1029/2018GL077801

The September 10-12 Solar Energetic Particle (SEP) Event produced the strongest increase of the radiation environment measured by the Radiation Assessment Detector (RAD) on the surface of Mars since landing in August 2012. We report the details of the measurements of the energetic particle environment from RAD in Gale crater during this event. The SEP event increased the low-energy proton flux (below 100 MeV) by a factor of thirty, and the higher-energy proton flux by a factor of four, above pre-event levels. The ^{4}He flux (below 100 MeV/nuc) rose by factors up to ten, and neutral particles by a factor of two above background. The increase started on September 10 around 19:50 UTC, peak-level fluxes were reached on the morning of September 11 and prevailed for about 10 hours before decreasing towards background levels. The onset of a Forbush decrease on September 13 decreased the proton flux below pre-event intensities.

Keypoints:

- On 11 Sept 2017, RAD observed the strongest solar particle event on the Martian surface since landing.
- Proton fluxes at the Martian surface increased by factors of up to thirty, helium fluxes by factors up to 10.
- Doubling of neutral particle environment has importance for planning of future storm shelter shielding, which is not as effective against neutrons compared to charged particles.

1. Introduction

Exposure to radiation from energetic particles remains one of the major health risks for astronauts on future exploration mission to the planet Mars. Assessing the expected radiation environment on the surface of Mars is, thus, of vital importance. The Martian surface radiation field differs greatly from the one on Earth for two main reasons: (1) Mars lacks a global magnetic field; (2) the Martian atmosphere is very thin (two orders of magnitude less atmospheric depth than Earth). This provides only weak shielding from impeding energetic particles. The resulting higher levels of radiation exposure on Mars pose a risk to the health of future human explorers, such as DNA damage or strand breaks, cancer, or cell death with potential fatal effects [*Baumstark-Khan and Facius*, 2001].

The Martian surface radiation environment is dominated by Galactic Cosmic Rays (GCRs) and secondary particles created by GCRs interacting with the nuclei of the atmosphere and soil. GCRs are very high energy particles and are composed of 98% atomic nuclei and 2% electrons. The nuclei divide into ∼87% protons, 12% helium, and 1% heavier nuclei [*Simpson*, 1983]. The GCRs can propagate deep into the thin Martian atmosphere, during which they can interact with the atmospheric nuclei creating secondary particles that also can propagate further down. GCRs can reach the surface and traverse into the soil. They can interact with the nuclei there producing secondary particles that propagate back to the surface. This creates a diverse surface radiation environment of charged and neutral particles [*Ehresmann et al.*, 2014; *Köhler et al.*, 2014], that needs to be monitored and understood to its full exent.

The Radiation Assessment Detector (RAD) [*Hassler et al.*, 2012] is an instrument on board the Curiosity rover on NASA's Mars Science Laboratory (MSL) mission [*Grotzinger et al.*, 2012]. RAD has been measuring the radiation environment at the surface of Gale crater on Mars since August 2012 [*Hassler et al.*, 2014; *Köhler et al.*, 2014; *Ehresmann et al.*, 2014; *Rafkin et al.*, 2014; *Guo et al.*, 2015]. RAD measures integral fluxes of charged particles for different ion species as described in more detail in [*Ehresmann et al.*, 2014]. In addition, RAD is capable of measuring differential energy spectra for single ion species and some isotopes (e.g., separate fluxes for protons, deuterons, and tritons) for particles with low enough energies to stop in the RAD detectors. Measured neutral particles can be distinguished into neutron and gamma-ray spectra via an inversion process [*Köhler et al.*, 2014]. These flux and spectra measurements provide important input to validate radiation transport models, such as High Charge and Energy Transport (HZETRN) [*Slaba et al.*, 2010] or Geometry and Tracking 4 (GEANT4) [*Agostinelli and the Geant4 Collaboration*, 2003], that are used to calculate the expected radiation environment and exposures for exploration missions.

While the radiation environment is mainly induced by GCRs, on shorter time scales it can be dominated by Solar Energetic Particles (SEPs) emitted from the Sun and accelerated during solar flares or in shocks associated with Coronal Mass Ejections (CMEs). These SEP events usually last for several days showing a rapid increase in the radiation environment with the arrival of the accelerated SEPs followed by a gradual decrease back to (or below) the previous level. For typical Martian atmospheric depths of around 20 g/cm^2, only protons with a least 150 MeV of initial energy will reach the surface. Parti-

cles with lower energies will be stopped in the atmosphere, predominantly by ionization energy loss. Thus, only SEP events where particles are accelerated to energies above this threshold can be directly detected on the surface of Mars. Model calculations show that those events can potentially increase the Martian surface radiation environment by orders of magnitude [*Gronoff et al.*, 2015; *Guo et al.*, 2018]. Here, not only the total accumulated radiation exposure during the whole event poses health risks, but also the very short-term, most intense radiation dose imparted during the peak times of the event, particularly if there is no additional shielding available (e.g., from a habitat).

SEP events can show a wide variety of spectral shapes and intensities, and their time of occurrence is hard to predict. Thus, to assess SEP-related health risks for human exploration, long-term monitoring of the effects of SEPs on the Martian surface radiation environment is essential. RAD measurements provide valuable information to better understand SEP propagation from the source to Mars, in particular as there are currently no dedicated energy-spectral measurements available in Martian orbit.

During the first five years of its mission, RAD detected five modest SEP events on the Martian surface (in April and October 2013, January and September 2014, and October 2015). A sixth event was detected on September 11 2017 and is the focus of this manuscript. The event occurred in the declining phase of solar cycle 24, when solar activity increased suddenly, starting from Active Region (AR) 12673, in the days leading up to September 10 2017. The AR produced several X-class flares, including an X8.2 flare on September 10. A few hours after the flare, RAD detected an increase in the surface radiation environment at around 19:50 UTC. The September 2017 event is of particular

interest because it was not only detected by RAD on the surface of Mars, but also by other instruments in orbit (see publications in this special issue). Furthermore, it was detected in Low-Earth Orbit (LEO) on the ISS, and with neutron monitors on the surface of Earth, making it the first Ground-Level Enhancement (GLE) SEP event observed simultaneously on two planets.

In this manuscript, we focus on RAD measurements of the energetic particle environment on the surface of Mars during the September 2017 SEP event. These data represent the first reported detection of a SEP event with the RAD instrument on Mars, making it a unique and highly important data set for the scientific community. We describe the evolution in intensity and time of the Martian surface proton fluxes, and calculate the differential stopping proton spectra (energies <100 MeV at the surface) for several time slices during the event. Furthermore, this SEP event produced a significant enhancement of the surface ^{4}He flux detectable in RAD data. We also describe changes in the neutral particle environment induced by SEP interactions with the atmospheric nuclei. These first-ever in-situ measurements of SEP spectra on Mars are expected to improve our understanding of both the propagation of SEPs from the Sun to Mars, as well as their transport through the Martian atmosphere.

2. Methods

To analyze the impact of the September 2017 event on the energetic particle environment on the surface of Mars, we use data acquired with the RAD instrument in Gale crater during the event. A detailed description of the RAD instrument and its calibration is given in [*Hassler et al.*, 2012; *Zeitlin et al.*, 2016].

2.1. The Radiation Assessment Detector

The RAD sensor head (RSH) consists of the following detectors: Three thin, and segmented Si diodes (named A, B, C) form the top of the detector stack, followed by a CsI scintillator D, and a plastic scintillator E below. A further plastic scintillator F surrounds D and E.

For charged particle measurements, the Si diodes A and B define the acceptance angle or Field-of-View (FOV) for incoming particles. The segmentation of A results in two FOVs: the inner one with full angle $\overline{\mathrm{A2B}} = 36°$, and a larger FOV spanned by the whole of A and B ($\overline{\mathrm{AB}} = 60°$). We distinguish two groups of charged particles. Penetrating particles have enough energy to pass through the whole detector stack (A through F) and exit the RSH. For these particles, we use the $\overline{\mathrm{A2B}}$ FOV to ensure a proper flight path through the bottom sides of D and E. Stopping particles can enter the RSH through either segment of detector A, but they must deposit all of their initial energy during their path through the detector stack. For this the particles must stop in the inner segments of B or C, or in the scintillator D. Stopping protons must have had roughly less than 100 MeV of energy. To penetrate the whole RSH, protons on average need more than $\sim$ 135$\pm$15 MeV (see [*Ehresmann et al.*, 2017]). These values refer to energies at the surface of Mars. Neutral particles are recorded in the D and E scintillators, with C and F acting as a surrounding anti-coincidence to veto charged particle signals.

2.2. Derived RAD data sets

For our analysis of the September 2017 SEP event, we are foremost interested in changes in the proton environment. Protons are the most dominant charged particle species on the

surface of Mars [*Ehresmann et al.*, 2017], both during solar quiet times when the radiation environment is dominated by GCRs, as well as during solar events where mainly protons are accelerated to high enough energies to reach the surface. The RAD measurements can be analyzed for penetrating and stopping charged particles, which then can be further filtered to select protons as described in detail in [*Ehresmann et al.*, 2014]. Folding these proton counts with the instrument's geometric factor, acquisition time, and other measurement-specific scaling factors, we can calculate integral proton fluxes based on the updated methods described in [*Ehresmann et al.*, 2017]. Since we know the total amount of energy stopping protons had at the surface of Mars, we can then also derive differential fluxes or energy spectra for these lower energy protons.

The same methods can be applied to derive fluxes for higher-Z particles (so-called HZEs). This is of interest for this research as during some SEP events there are significant increases in helium and other higher-Z ion fluxes detected in interplanetary space [see e.g. *Mewaldt et al.*, 2005]. If these HZEs reach Mars, they not only lose energy interacting with the atmospheric nuclei, there is also a probability that these ions will undergo fragmentation processes. Because of the overall lower abundances (than protons) of these HZEs, and the comparably small geometric factor of the compact RAD instrument, HZE SEPs can only be detected on the surface of Mars if they are accelerated to high enough energies with a significant increase in intensity during SEP events.

Neutral particles are created during interactions of incoming GCRs or SEPs with the nuclei of atmosphere and soil. Therefore, an increase in the primary radiation during a SEP event will lead to an increase in secondary (neutral) radiation. Monitoring the neutral

radiation is important as typical shielding scenarios for SEP events mainly include using additional shielding material ("storm shelters") to slow down and stop SEPs [*Clark*, 1993]. However, neutral particles have a low interaction probability with these shielding materials and their flux will, thus, not be decreased as strongly. To analyze this, we make use of RAD neutral particle counters, counting signals above threshold in the E scintillator in anti-coincidence with the surrounding detectors. While the counter does not provide the species or energy information for the neutral particles (which have to be derived via an inversion that requires high number of neutrals measured), it has the advantage to provide a data set with enough statistics on shorter time scales, such as during a SEP event.

In normal mode, RAD measurements are taken in separate $\sim$ 16 min observations in a 100% duty cycle. During times of high count rates, RAD switches into an "SEP" mode, doubling its cadence to 8 min observations.

3. Results

3.1. Martian surface proton fluxes

In the days before the first SEPs started to arrive at Mars, the penetrating proton surface flux (with proton energies $\sim$ higher than 135 MeV at the surface) was around 0.324 $\pm$0.052 cm^{-2} s^{-1} sr^{-1} (from here on called pfu or particle flux unit). RAD began seeing increases in the radiation dose on September 10 at around 19:50 UTC. "SEP" mode was triggered on September 11 at around 01:00 UTC and lasted until $\sim$ 05:00 UTC of the following day.

Figure 1 shows the penetrating and stopping proton fluxes versus time from 09/07/00:00UTC to 09/19/00:00UTC. Defining the timing of the first impact of SEPs

on the penetrating flux is limited by the small FOV of the $\overline{\text{A2B}}$ coincidence. Nonetheless, we find a first increase in flux above 3σ statistical significance at around UTC 21:50 of September 10. The increases before this time are below the 3σ level for the penetrating flux, and thus this time is slightly later than the increase in radiation dose, which is recorded with a higher geometric factor. The flux then increased from the previous 0.324 pfu by a factor of nearly 4 up to a value of 1.2 pfu (around 07:00 UTC on September 11) with highest intensities in the period between 04:00 to 14:00 UTC. The flux then decreased and dropped below pre-event level after the onset of the Forbush decrease (FD) around 02:51 UTC on September 13. The flux stayed below 0.250 pfu for several days, until it started to recover on September 16 reaching 0.275 pfu by the end of September 18.

Prior to the arrival of SEPs, the stopping proton surface flux (protons with less than $\sim$ 100 MeV at the surface) was 0.025 $\pm$0.006 pfu. The first increase in flux above 3σ significance occurred around 22:45 UTC on September 10, slightly later than for the penetrating flux, owing to the longer travel time of the slower protons. Binning the stopping data more finely shows that the flux in the lowest energy bin of 10-20 MeV increases even later, around 00:00 UTC. Similarly, the stopping flux increase also peaks later, reaching a maximum of 0.727 pfu on September 11 at around 09:00 UTC. Similarly high values persist until 14:00 UTC. Compared to solar quiet time, the stopping flux was a factor of 30 higher during the event, whereas the penetrating particle flux increased by a factor of 3-4 compared to quiet time. These trends are due to the fact that the initial SEP spectrum falls off with a power law above the 150 MeV needed to reach the Martian

surface. During the FD, the stopping proton flux dropped rapidly from above 0.1 pfu to below 0.04 pfu between 04:40 and 05:40 UTC on September 13.

3.2. Stopping proton spectra

The differential flux measurements of stopping protons are of particular interest for transport model validation, where the model output for a given input spectrum can be directly compared to the flux per energy. In Figure 2, we provide spectra measured over 6 hours each, starting on September 11 at 00:00 UTC while SEP fluxes were rising quickly, and ending on September 13 00:00 UTC before the onset of the FD. The separate spectra are shown in 10 MeV bins spanning 10 to 90 MeV. The figure also shows the average pre-event proton flux from September 7-10 (black).

All spectra should be interpreted as containing GCR and SEP contributions. It can be seen that in the rising phase of the event (00:00-06:00 UTC on September 11), the spectrum is already more than an order of magnitude higher than pre-event levels. We can't identify any significant changes of the spectral shape of the surface flux over time, which could have indicated differences in the spectral shape of the incoming SEP particles. The presented data provide particularly valuable input when modeling the SEP propagation to Mars and down to the surface, as they can be used as time-dependent ground-truth data for the model calculations.

3.3. Increase in helium-4 surface flux

Detecting HZE SEP enhancements on the surface of Mars is challenging. During solar quiet times, when the HZE surface flux is due to GCRs, RAD typically records single-digit HZE counts per observation, due to the low abundances of these ions and the small

geometric factor of the instrument. In the stopping energy range which SEPs would preferentially populate, GCR counts can average less than 1 per observation. Therefore, for RAD to detect a statistically significant signal during a SEP event, HZE particles must be accelerated to significantly high energies with high intensities, to overcome the decrease of intensity with increasing radial distance from the Sun, transport losses in the atmosphere, and the small geometric factor. Nonetheless, the strength of the September 2017 GLE event allows us to report for the first time a significant increase in part of the HZE population on the Martian surface, specifically, the stopping ^{4}He flux (with surface energies below 100 MeV/nuc).

Figure 3 shows the integral stopping particle flux of ^{4}He (surface energies below 100 MeV/nuc) versus time. The data are binned in 6-hour observations to reduce statistical uncertainty in the counts to below 20% in the peak period.

In the peak intensity time bin (September 11 06:00-12:00 UTC), the flux rises to $4.4{\cdot}10^{-3}$ pfu, a factor of 7-10 above the pre-event level flux ($4.5\text{-}6.5{\cdot}10^{-4}$ pfu). There appear to be no significant changes in the flux values in the time from September 11 12:00 UTC to September 12 06:00 UTC, followed by a steep decrease to the next observation point when the spectrum flattens out. After the onset of the FD on September 13, the flux decreases to below $4{\cdot}10^{-4}$ pfu, slightly below pre-event levels. Although these first ^{4}He SEP measurements suffer from low statistics, they can provide valuable input for the analysis of higher-Z SEP propagation.

3.4. Increase in neutral particle counts

The current approach to shield astronauts from the radiation impacts of SEP events are so-called storm shelters. These are places in a spacecraft or planetary habitat that provide an increased amount of shielding material to stop the SEP protons. As we see on Mars, $\sim$20 g/cm^2 of atmospheric shielding "material" will stop protons with energies below 150 MeV in the atmosphere. As seen in the RAD proton data presented here, the highest intensity increase for SEP particles is for protons with energies below 100 MeV on the surface. A storm shelter of several cm of material is therefore a reasonable approach. This depends on the timing of the warning system and the intensity of the SEP event. Events with intensities orders of magnitude higher than this event are possible, and might require additional safety measures.

One must additionally consider the increase in secondary neutral radiation during an SEP event. Neutrons, in particular, are of high biological relevance, and have a low interaction cross section with common shielding materials. Interactions of SEPs and shielding material can then produce additional neutrons. To analyze, we used the RAD neutral particle counter for detector E L2[6] [*Zeitlin et al.*, 2016]. As noted, the RAD L2[6] counter of detector E records both neutrons and gamma-rays. However, due to its high hydrogen content E is much more susceptible to neutrons which contribute most of the counts (see Figure 3 in [*Köhler et al.*, 2014]). [*Guo et al.*, 2017] have furthermore calculated that around 88% of the neutral dose recorded in E is from neutrons. Therefore, to first order the L2[6] count rate can give a good indication of the increase in neutron radiation during this SEP event.

Figure 4 shows the count rate versus time for 09/10 00:00 UTC to 09/14 00:00 UTC. We find that the neutral particle counts increase later than the SEP protons. We detect the first increase above 3σ uncertainty on September 11 UTC around 01:45 UTC. The increase peaks at around 12:00 UTC later that day at a factor of 2 higher than the pre-event level. The decrease of the count rate after the peak period flattens out at around September 12 00:00 UTC until the onset of the FD. Assuming the increase in neutral count rate correlates with an increase in neutron flux, this shows that the neutron radiation environment might double during the peaks of SEP events, with the potential to traverse any additional storm-shielding material.

4. Discussion

This manuscript presents measurements of the energetic particle radiation environment on the surface of Mars during the September 2017 solar event as observed by the MSL/RAD instrument in Gale crater. These RAD measurements of integral and differential particle fluxes are directly relevant for the validation of radiation transport codes used to model expected radiation exposure on deep-space and planetary exploration missions and serve as important input to assist with the planning of future human exploration of Mars.

The solar energetic particles arriving at Mars during the September 10-12 event had high enough energies to penetrate the Martian atmosphere and increase the surface proton environment by a factor of 30 for protons with energies below 100 MeV, and a factor of 4 for energies above $\sim$ 135 MeV, yielding the highest such increases recorded by RAD since landing on Mars in 2012. The strong SEP event also led to discernible rise by factors up to

10 in the low-energy ^{4}He flux (below 100 MeV/nuc). Analysis of the RAD neutral particle counters also shows a doubling of the neutral radiation environment during the peak event time. Monitoring the increase in neutron radiation can be particularly important for planning future shielding measures, such as high-mass storm shelters, which do not shield neutrons with as high of an efficiency as charged particles. We further analyzed the differential proton flux (below 100 MeV) over the duration of the event and do not find significant changes in the spectral shape that could have indicated a softening or hardening of the SEP spectrum above the Martian atmosphere over time.

The results reveal interesting scientific questions for future research. It is not well understood why the neutrals show a delay in timing compared to the charged particles. Noteable is also that ^{4}He- and neutral signals flatten out in the decreasing phase of the event. Deriving a spectral index for the SEPs in orbit from RAD data can increase our understanding of SEP propagation in the heliosphere. The complexity of these analyses would exceed the concise nature of this manuscript, which therefore focuses on the actual measurements.

Acknowledgments. RAD is supported by NASA (HEOMD) under Jet Propulsion Laboratory (JPL) subcontract #1273039 to Southwest Research Institute and in Germany by the German Aerospace Center (DLR) and DLR's Space Administration grant numbers 50QM0501, 50QM1201, and 50QM1701 to the Christian-Albrechts-Universität zu Kiel. The data used in this paper are archived in the NASA Planetary Data Systems Planetary Plasma Interactions Node at the University of California, Los Angeles. The archival volume includes the full binary raw data files, detailed descriptions of the structures

therein, and higher-level data products in human-readable form. The PPI node is hosted at the following URL: http://ppi.pds.nasa.gov/.

References

Agostinelli, S., and the Geant4 Collaboration (2003), Geant4-a simulation toolkit, *Nuclear Instruments and Methods in Physics Research A*, *506*, 250–303.

Baumstark-Khan, C., and R. Facius (2001), *Life under conditions of ionizing radiation. In: Astrobiology. The Quest for the Conditions of Life.*, pp. 260–283, Springer Verlag.

Clark, B. C. (1993), *Radiation Protection for Human Interplanetary Spaceflight and Planetary Surface Operations*, pp. 871–888.

Ehresmann, B., C. Zeitlin, D. M. Hassler, R. F. Wimmer-Schweingruber, E. Böhm, S. Böttcher, D. E. Brinza, S. Burmeister, J. Guo, J. Köhler, C. Martin, A. Posner, S. Rafkin, and G. Reitz (2014), Charged particle spectra obtained with the Mars Science Laboratory Radiation Assessment Detector (MSL/RAD) on the surface of Mars, *Journal of Geophysical Research (Planets)*, *119*, 468–479, doi:10.1002/2013JE004547.

Ehresmann, B., C. J. Zeitlin, D. M. Hassler, D. Matthiä, J. Guo, R. F. Wimmer-Schweingruber, J. K. Appel, D. E. Brinza, S. C. Rafkin, S. I. Böttcher, S. Burmeister, H. Lohf, C. Martin, E. Böhm, and G. Reitz (2017), The charged particle radiation environment on mars measured by msl/rad from november 15, 2015 to january 15, 2016, *Life Sciences in Space Research*, *14*, 3 – 11, doi:https://doi.org/10.1016/j.lssr.2017.07.004, radiation on the Martian Surface: Model Comparisons with Data from the Radiation Assessment Detector on the Mars Science Laboratory (MSL/RAD): Results from the 1st Mars Space Radiation Modeling Workshop.

Gronoff, G., R. B. Norman, and C. J. Mertens (2015), Computation of cosmic ray ionization and dose at mars. i: A comparison of {HZETRN} and planetocosmics for proton and alpha particles, *Advances in Space Research*, pp. –, doi: http://dx.doi.org/10.1016/j.asr.2015.01.028.

Grotzinger, J. P., J. Crisp, A. R. Vasavada, R. C. Anderson, C. J. Baker, R. Barry, D. F. Blake, P. Conrad, K. S. Edgett, B. Ferdowski, R. Gellert, J. B. Gilbert, M. Golombek, J. Gómez-Elvira, D. M. Hassler, L. Jandura, M. Litvak, P. Mahaffy, J. Maki, M. Meyer, M. C. Malin, I. Mitrofanov, J. J. Simmonds, D. Vaniman, R. V. Welch, and R. C. Wiens (2012), Mars Science Laboratory Mission and Science Investigation, *Space Sci. Rev.*, *170*, 5–56, doi:10.1007/s11214-012-9892-2.

Guo, J., C. Zeitlin, R. F. Wimmer-Schweingruber, S. Rafkin, D. M. Hassler, A. Posner, B. Heber, J. Köhler, B. Ehresmann, J. K. Appel, E. Böhm, S. Böttcher, S. Burmeister, D. E. Brinza, H. Lohf, C. Martin, H. Kahanpää, and G. Reitz (2015), Modeling the Variations of Dose Rate Measured by RAD during the First MSL Martian Year: 2012-2014, *The Astrophysical Journal*, *810*(1), 24.

Guo, J., C. Zeitlin, R. Wimmer-Schweingruber, D. M. Hassler, J. Köhler, B. Ehresmann, S. Böttcher, E. Böhm, and D. E. Brinza (2017), Measurements of the neutral particle spectra on mars by msl/rad from 2015-11-15 to 2016-01-15, *Life Sciences in Space Research*, *14*, 12 – 17, doi:https://doi.org/10.1016/j.lssr.2017.06.001, radiation on the Martian Surface: Model Comparisons with Data from the Radiation Assessment Detector on the Mars Science Laboratory (MSL/RAD): Results from the 1st Mars Space Radiation Modeling Workshop.

Guo, J., C. Zeitlin, R. F. Wimmer-Schweingruber, T. McDole, P. Kühl, J. C. Appel, D. Matthiä, J. Krauss, and J. Köhler (2018), A generalized approach to model the spectra and radiation dose rate of solar particle events on the surface of mars, *The Astronomical Journal*, *155*(1), 49.

Hassler, D. M., C. Zeitlin, R. F. Wimmer-Schweingruber, S. Böttcher, C. Martin, J. Andrews, E. Böhm, D. E. Brinza, M. A. Bullock, S. Burmeister, B. Ehresmann, M. Epperly, D. Grinspoon, J. Köhler, O. Kortmann, K. Neal, J. Peterson, A. Posner, S. Rafkin, L. Seimetz, K. D. Smith, Y. Tyler, G. Weigle, G. Reitz, and F. A. Cucinotta (2012), The Radiation Assessment Detector (RAD) Investigation, *Space Sci. Rev.*, *170*, 503–558, doi:10.1007/s11214-012-9913-1.

Hassler, D. M., C. Zeitlin, R. F. Wimmer-Schweingruber, B. Ehresmann, S. Rafkin, J. L. Eigenbrode, D. E. Brinza, G. Weigle, S. Böttcher, E. Böhm, and et al. (2014), Mars' Surface Radiation Environment Measured with the Mars Science Laboratory's Curiosity Rover, *Science*, *343*, 1244797, doi:10.1126/science.1244797.

Köhler, J., C. Zeitlin, B. Ehresmann, R. F. Wimmer-Schweingruber, D. M. Hassler, G. Reitz, D. E. Brinza, G. Weigle, J. Appel, S. Böttcher, E. Böhm, S. Burmeister, J. Guo, C. Martin, A. Posner, S. Rafkin, and O. Kortmann (2014), Measurements of the neutron spectrum on the Martian surface with MSL/RAD, *Journal of Geophysical Research (Planets)*, *119*, 594–603, doi:10.1002/2013JE004539.

Mewaldt, R. A., C. M. S. Cohen, A. W. Labrador, R. A. Leske, G. M. Mason, M. I. Desai, M. D. Looper, J. E. Mazur, R. S. Selesnick, and D. K. Haggerty (2005), Proton, helium, and electron spectra during the large solar particle events of october-

november 2003, *Journal of Geophysical Research: Space Physics*, *110*(A9), n/a–n/a, doi:10.1029/2005JA011038, a09S18.

Rafkin, S. C. R., C. Zeitlin, B. Ehresmann, D. Hassler, J. Guo, J. Köhler, R. Wimmer-Schweingruber, J. Gomez-Elvira, A.-M. Harri, H. Kahanpää, D. E. Brinza, G. Weigle, S. Böttcher, E. Böhm, S. Burmeister, C. Martin, G. Reitz, F. A. Cucinotta, M.-H. Kim, D. Grinspoon, M. A. Bullock, and A. Posner (2014), Diurnal variations of energetic particle radiation at the surface of Mars as observed by the Mars Science Laboratory Radiation Assessment Detector, *Journal of Geophysical Research (Planets)*, *119*, 1345–1358, doi:10.1002/2013JE004525.

Simpson, J. A. (1983), Elemental and Isotopic Composition of the Galactic Cosmic Rays, *Annual Review of Nuclear and Particle Science*, *33*, 323–382, doi:10.1146/annurev.ns.33.120183.001543.

Slaba, T. C., S. R. Blattnig, and F. F. Badavi (2010), Faster and more accurate transport procedures for HZETRN, *Journal of Computational Physics*, *229*, 9397–9417, doi:10.1016/j.jcp.2010.09.010.

Zeitlin, C., D. M. Hassler, R. F. Wimmer-Schweingruber, B. Ehresmann, J. Appel, T. Berger, E. Böhm, S. Böttcher, D. E. Brinza, S. Burmeister, J. Guo, J. Köhler, H. Lohf, C. Martin, D. Matthiä, A. Posner, S. Rafkin, G. Reitz, Y. D. Tyler, M. Vincent, G. Weigle, Y. Iwata, H. Kitamura, and T. Murakami (2016), Calibration and characterization of the radiation assessment detector (rad) on curiosity, *Space Science Reviews*, *201*(1), 201–233, doi:10.1007/s11214-016-0303-y.

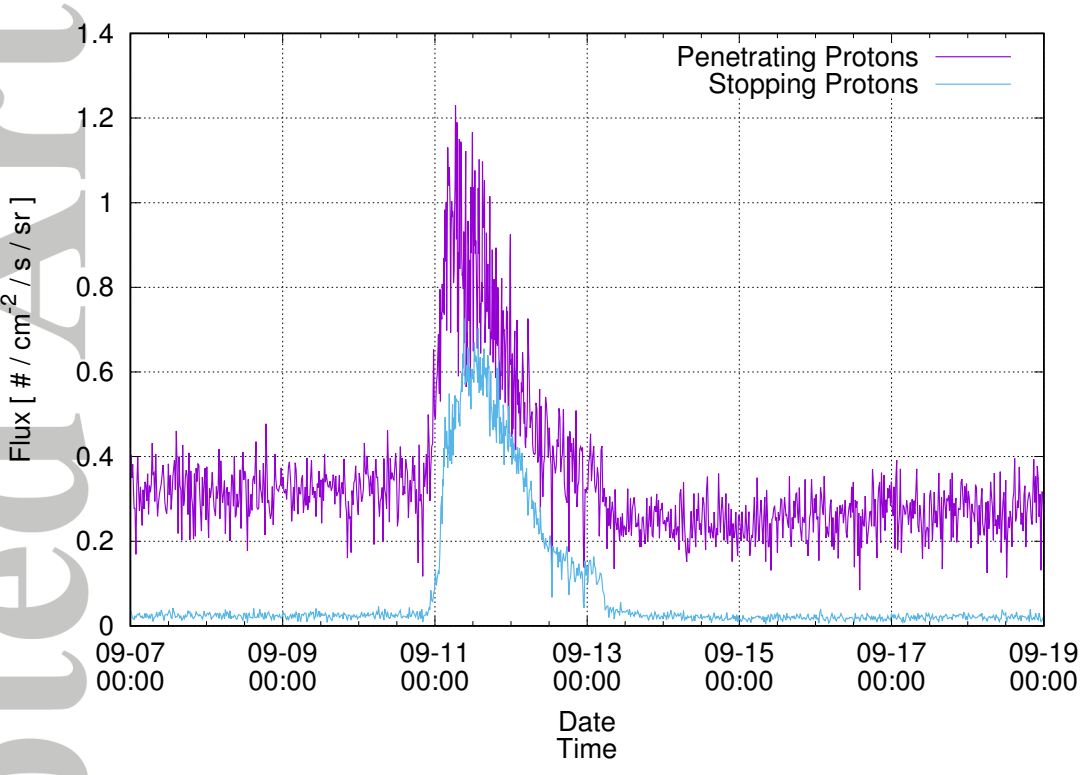

Figure 1. Integrated proton fluxes versus time. The penetrating flux (energies above $\sim$ 135 MeV) is shown in magenta, the stopping proton flux (below $\sim$ 100 MeV) in light blue.

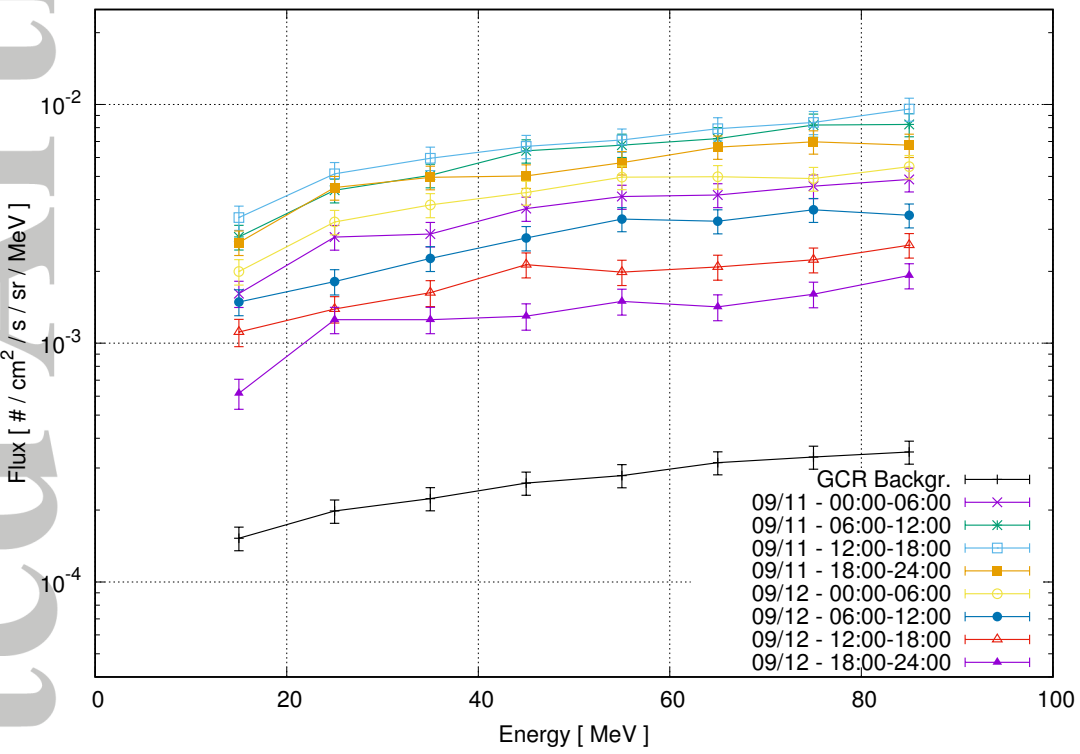

Figure 2. Differential flux spectra for stopping protons. Colors and symbols denote the spectra for the different observation times. As a reference, the GCR-induced proton spectrum from before the event is plotted in black.

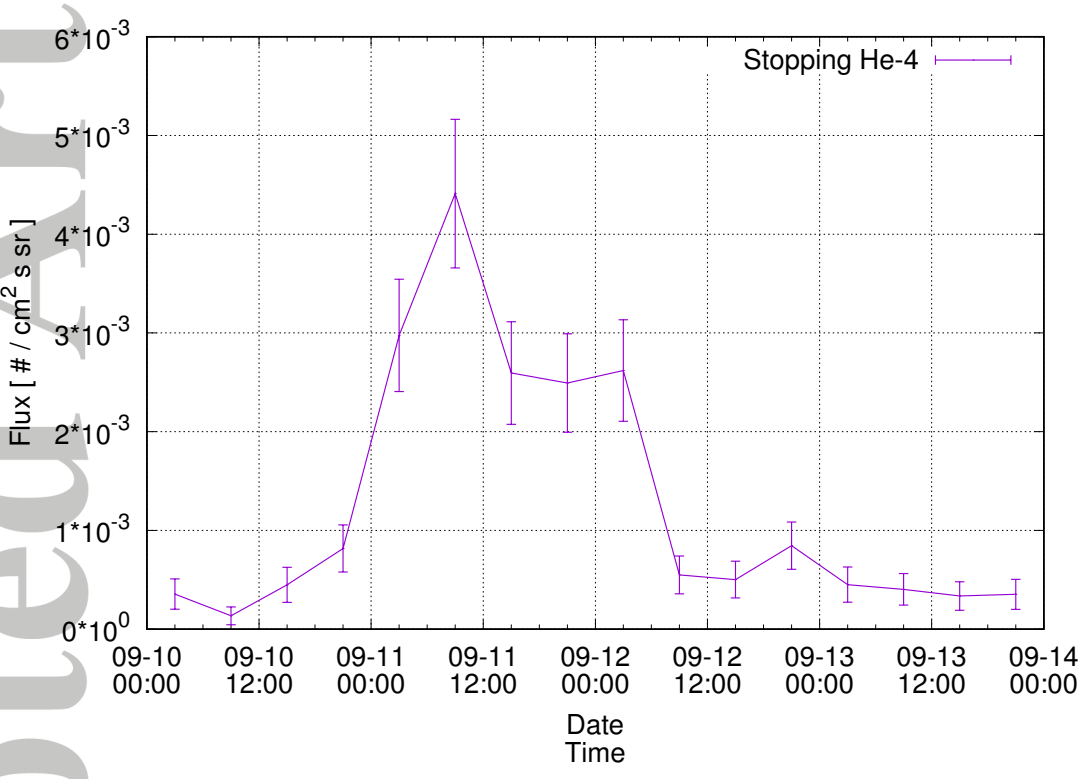

Figure 3. Integral stopping ^{4}He flux (smaller than 100 MeV/nuc) versus time. Data are binned into 6-hours of measurement.

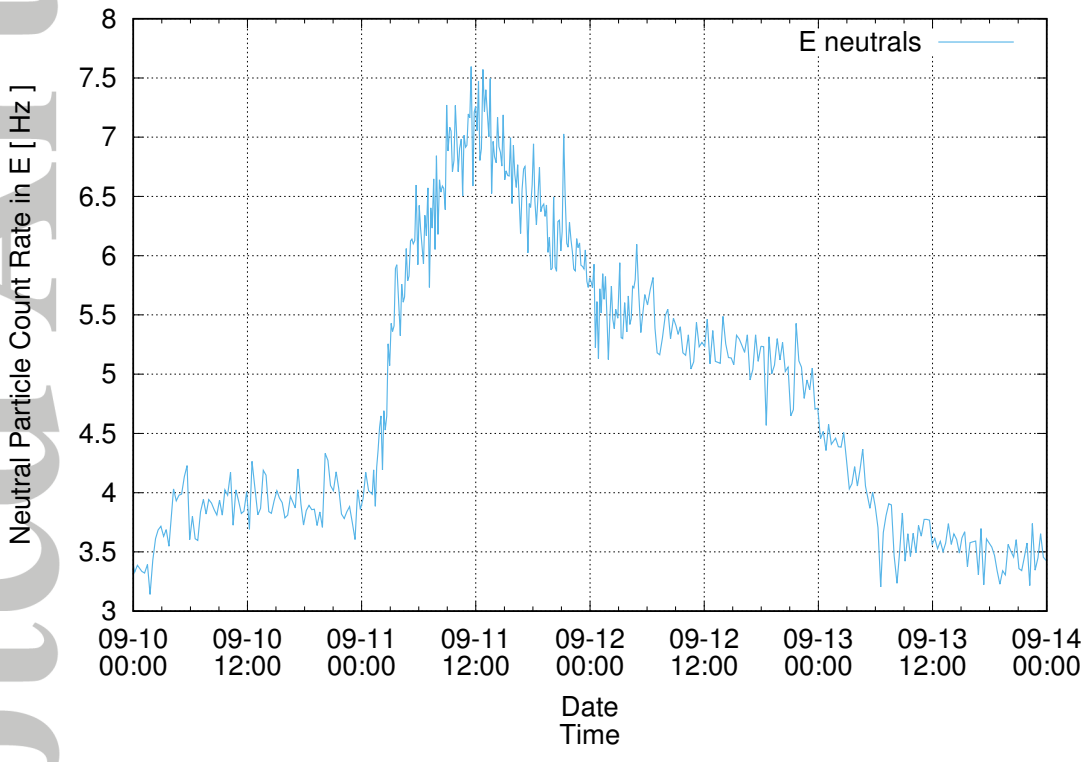

Figure 4. RAD L2[6] count rate versus time. L2[6] counts neutral particles in detector E.